

Carrier concentration dependence of optical Kerr nonlinearity in indium tin oxide films

Hendry Izaac Elim¹, Wei Ji^{1,*}, and Furong Zhu²

¹Physics Department, National University of Singapore, 2 Science Drive 3,
Singapore 117542

²Institute of Materials Research and Engineering, 3 Research Link, Singapore 117602

Abstract

Optical Kerr nonlinearity (n_2) in n -type indium tin oxide (ITO) films coated on glass substrates has been measured using Z -scans with 200-fs laser pulses at wavelengths ranging from 720 to 780 nm. The magnitudes of the measured nonlinearity in the ITO films were found to be dependent on the carrier concentration with a maximum n_2 -value of $4.1 \times 10^{-5} \text{ cm}^2/\text{GW}$ at 720-nm wavelength and an electron density of $N_d = 5.8 \times 10^{20} \text{ cm}^{-3}$. The Kerr nonlinearity was also observed to be varied with the laser wavelength. By employing a femtosecond time-resolved optical Kerr effect (OKE) technique, the relaxation time of OKE in the ITO films is determined to be ~ 1 ps. These findings suggest that the Kerr nonlinearity in ITO can be tailored by controlling the carrier concentration, which should be highly desirable in optoelectronic devices for ultrafast all-optical switching.

PACS 42.65.An; 42.65.Hw; 78.40.Fy

*E-mail address: phyjiwei@nus.edu.sg

1 Introduction

Thin films of transparent conducting oxide (TCO) have increasingly attracted attention because they are both electrically conductive and optically transparent in the visible wavelength range. The unique combination of such desirable electrical and optical properties makes TCO films directly relevant to various applications in electronics and optoelectronics [1, 2]. Among many TCOs, indium tin oxide (ITO) is one of the most frequently utilized materials in practical optoelectronic devices. ITO films may be fabricated by many methods, including reactive thermal evaporation deposition, magnetron sputtering, electron beam evaporation, spray pyrolysis, and chemical vapor deposition [3-9]. The optical transparency and electrical conduction mechanism of ITO films have been studied extensively, and important fabrication parameters that control the electrical conductivity of ITO films have been described in detail in Refs [3, 10, 11].

However, the material properties of ITO films have not been fully understood yet, in particular, with regard to the third-order nonlinear-optical properties. Recently, large photo-conductivity in another TCO material, ZnO thin film, has been reported [12], implying that TCOs should possess large optical nonlinearities. In addition, the concentration of free charged carriers (electrons in the conduction band and holes in the valence band) plays a significant role in the electrical conductivity; and as expected, the free-charged-carrier density should influence optical nonlinearities as well, in particular, optical Kerr nonlinearity which is proportional to the light irradiance with the proportionality denoted as n_2 . Optical Kerr nonlinearity is of direct relevance to all-optical switching devices. Here we report our investigation into optical Kerr nonlinearity in ITO thin films and its dependence on the free-charged-carrier density.

2 Experimental arrangements

The nonlinear optical measurements were conducted in the transparent wavelength region by using 200-fs laser pulses at wavelengths ranging from 720 to 780 nm. The ITO films used in the measurements were prepared by a radio frequency magnetron sputtering method described below. An oxidized target with In_2O_3 and SnO_2 in a weight ratio of 9:1 was employed for the ITO film deposition. The substrate was not heated during and after the film deposition. Sputtering power was kept constant at 100 W. The base pressure in the sputtering system was approximately 2.0×10^{-4} Pa. During the film deposition, the argon-hydrogen gas mixture was employed. The argon partial pressure was set as 2.9×10^{-1} Pa, and the hydrogen partial pressure was controlled (from 1.1×10^{-3} to 4.0×10^{-3} Pa) to modulate and optimize the properties of ITO films [13]. Each film was grown on a substrate which consisted of a 1-mm-thick glass coated SiO_2 thin film. The film thickness of the ITO films was ranging from 118 to 138 nm, as shown in Table 1. Both Hall effect and Seebeck measurements revealed that these films were *n*-type semiconductors and the free-charged-carrier concentrations were varied with the growth conditions. The carrier concentrations of four samples used in the Z-scan measurements discussed below were determined to be 4.0×10^{20} , 4.4×10^{20} , 5.4×10^{20} , and $5.8 \times 10^{20} \text{ cm}^{-3}$. They are labeled as ITO-2, ITO-3, ITO4, and ITO-5 respectively.

3 Results and discussion

Figure 1 displays the transmission spectra of the ITO films, showing that the transparency of the four samples was between 85% and 89% in the spectral region of 700~900 nm. The plots in the inset of Fig. 1 illustrate that the indirect-band-gap energies

of the ITO films are located between 3.05 and 3.15 eV, depending on the carrier concentration. As shown in Table 1, the indirect-band-gap energy increases as the free-charged-carrier density rises. It is in agreement with the report by Zhang *et al.* [9]. This dependence is also known as Moss-Burstein shift due to band-gap re-normalization through many-body effects.

To investigate the optical Kerr nonlinearity in the ITO films at room temperature, we employed the Z-scan technique [14] with 200-fs-laser pulses at 1 kHz pulse repetition rate. The laser pulses were generated by a mode-locked Ti:Sapphire laser (Quantronix, IMRA), which seeded a Ti:Sapphire regenerative amplifier (Quantronix, Titan). The laser wavelengths were tunable from 720 to 780 nm (1.72 to 1.59 eV), by feeding the output from the Ti:Sapphire regenerative amplifier to an optical parametric amplifier (TOPAS, Light Conversion, Quantronix). The laser pulses were focused and the sample was Z-scanned across the focal point. By using a set of neutral density filters, the laser irradiances can be varied from a few to 300 GW/cm² at the focal point.

To eliminate the contribution from glass substrates, we first performed Z-scans on a glass substrate coated with a 200-nm-thick layer of SiO₂. Figure 2(a) and (b) display a photo-bleaching signal and positive Kerr nonlinearity (n_2), respectively, for the substrate. The photo-bleaching in crystalline and amorphous SiO₂ has been studied extensively. Recent investigation by Sasajima and Tanimura [15] revealed that the optical bleaching can be attributed to one-center self-trapping holes peaked at 2.16 eV and two-center self-trapping holes for the 2.60-eV band, though the nature of the local distortion that induces the supplemental potential for hole localization is still unclear. Assuming that the absorption coefficient may be expressed as $\alpha_0 + \alpha_2 I$, where α_0 is the linear absorption

coefficient, α_2 the nonlinear absorption coefficient, and I the light irradiance, we employ the Z-scan theory [14] to simulate the open-aperture Z-scan data. The best-fit solid line in Fig. 2(a) infers that α_2 is -1×10^{-5} cm/GW for the substrate.

Figure 2(a) and (b) also illustrate typical open- and close-aperture Z-scans for Sample ITO-5. It is interesting to notice the flat data (within our experimental errors) for the open-aperture Z-scan and the symmetric data for the closed-aperture Z-scan, indicating that absorptive nonlinearity vanishes ($\alpha_2 \sim 0$). We believe that the photo-beaching in the substrate should be cancelled out by the two-photon absorption in the ITO film. The two-photon energy ($2h\nu = 3.44$ eV for $\lambda = 720$ nm) is greater than the indirect-band-gap energy ($3.05 \sim 3.15$ eV) of the ITO films. We estimate the two-photon absorption coefficient, β , for the ITO-5 film by $\beta = -\alpha_2 L_{\text{substrate}} / L_{\text{ITO}} \sim 0.1$ cm/GW, where $L_{\text{substrate}}$ and L_{ITO} are the thickness of the substrate and the ITO film, respectively. Unfortunately, the theoretical value for β is unavailable in literature for ITO. However, for indirect-band-gap semiconductor GaP ($E_g^{\text{ind}} \approx 2.3$ eV) the theoretical β -value is reported to be ~ 0.5 cm/GW [16], which is close to our finding for ITO.

Although the resultant nonlinear absorption disappears for the ITO film on the substrate, the resultant nonlinear refraction is enhanced due to the same sign for the Kerr nonlinearity in both the substrate and the ITO film. The difference between the two Z-scans in Fig. 2(b) looks marginal, but the n_2 parameter of the ITO-5 film is much greater than the substrate if the 133-nm thickness of the ITO-5 film is compared to the 1-mm thickness of the substrate. By using the Z-scan theory [14] with the total refractive index expressed as $n_0 + n_2 I$, where n_0 is the linear refractive index, we numerically compute the close-aperture Z-scans with n_2 being an adjustable parameter. The n_2 value is extracted by

the theoretical curve that best fits to the data. For the substrate, we find that n_2^{sub} is 1.6×10^{-13} esu (or 4.8×10^{-7} cm²/GW) at 720 nm, close to $\sim 1.1 \times 10^{-13}$ esu measured at 1.064 nm by Adair *et al.* [17]. For the ITO film coated on the substrate, the total nonlinear magnitude (n_2L) is first extracted from the best-fit Z-scan curve; and then n_2^{ITO} is inferred by $n_2^{ITO} = (n_2L - n_2^{sub}L_{substrate})/L_{ITO}$. Similar experiments and data analyses were carried out for other three wavelengths: 730, 750 and 780 nm. Figure 2(c) displays a typical close-aperture Z-scan for 780 nm while the Z-scan measured at 720 nm is used as a reference. The Kerr nonlinearity in the ITO-5 film was determined to be 4.1×10^{-5} cm²/GW at 720 nm, 1.2×10^{-5} cm²/GW at 730 nm, 0.8×10^{-5} cm²/GW at 750 nm, and 0.6×10^{-5} cm²/GW at 780 nm. The Z-scans were also conducted at various excitation irradiances. In Fig. 3(a), the n_2^{ITO} values are plotted as a function of the excitation irradiance, which clearly indicates that the observed nonlinearity is of cubic nature. Other three samples (ITO-2, ITO-3, and ITO-4) were investigated in a similar fashion. Their Kerr nonlinearity is summarized in Table 1 while Fig. 3(b) shows the carrier density dependence. Such dependence has been observed in indirect-band-gap semiconductors like Si and Ge [18] and explained by free-electron theory [18]. However, no explicit theoretical calculation has been developed for ITO films yet. Our observation confirms a linear dependence, which has been predicted by the free-electron theory for the low carrier-concentration regime in Si and Ge [18].

To evaluate the relaxation time and to gain an insight of the underlying mechanism for the observed cubic nonlinearities, we conducted a time-resolved optical Kerr effect (OKE) experiment at 780 nm with the use of 200-fs laser pulses from the femtosecond laser system described previously. Figure 4(a) illustrates the transient OKE

signals as a function of the delay time for the substrate and Sample ITO-5 at a pump irradiance of 8.5 GW/cm^2 . The transient signals clearly shows there are two components. By using a two-exponential-component model, the best fits (solid lines in Fig. 4(a)) produce $\tau_1 = \sim 200 \text{ fs}$ and $\tau_2 = \sim 1 \text{ ps}$. We believe that τ_1 is the autocorrelation of the laser pulses used. The τ_2 component is the recovery time of the excited electrons in the ITO-5 sample. From the OKE signals at zero delay time, the magnitude of the third-order nonlinear susceptibility ($\chi^{(3)}$) of the sample is given by [19]

$$|\chi_s^{(3)}| \approx |\chi_r^{(3)}| \left(\frac{F_s}{F_r} \right)^{1/2} \left(\frac{n_0^s}{n_0^r} \right)^2 \left(\frac{L_r}{L_s} \right) \left(\frac{1-R_r}{1-R_s} \right)^{3/2} \left(\frac{\alpha_0^s L_s}{\exp\left(-\frac{1}{2}\alpha_0^s L_s\right)[1-\exp(-\alpha_0^s L_s)]} \right) \quad (1)$$

where F is the magnitude of OKE signal, L the interaction length, R the surface reflectance, α_0 the linear absorption coefficient, and n_0 the linear refractive index. The subscripts s and r denote the ITO-5 sample and the substrate, respectively. As for the substrate (reference sample), the value of n_2 is $1.6 \times 10^{-13} \text{ esu}$ or $\text{Re } \chi^{(3)} = \sim 2.5 \times 10^{-14} \text{ esu}$; and the value of α_2 is $-1 \times 10^{-5} \text{ cm/GW}$ or $\text{Im } \chi^{(3)} = \sim -0.5 \times 10^{-14} \text{ esu}$, which were measured in the above-discussed Z-scans. Therefore, $|\chi_r^{(3)}| = \sqrt{(\text{Im } \chi^{(3)})^2 + (\text{Re } \chi^{(3)})^2}$ is $2.8 \times 10^{-14} \text{ esu}$. Through use of this reference value, the magnitude of $|\chi_s^{(3)}|$ for the ITO-5 sample is determined to be $1.1 \times 10^{-12} \text{ esu}$. This $\chi^{(3)}$ is two orders of magnitude larger than that of the substrate, in agreement with our Z-scan data. On the other hand, Fig. 4(b) displays the time-resolved OKE signals obtained from Sample ITO-5 at the same wavelength with three different pump irradiances. The linear dependence of the OKE

signals on the excitation irradiance confirms the nature of third-order nonlinear processes, consistent with our *Z*-scan studies.

4 Conclusions

In conclusion, we have observed the optical Kerr nonlinearity and its carrier concentration dependence in ITO films with femtosecond laser pulses. It should be pointed out that the observed Kerr nonlinearity makes ITO films promising for ultrafast all-optical switching. For an ITO film with an electron density of $N_d = 5.8 \times 10^{20} \text{ cm}^{-3}$, the figure of merit [$\text{FOM} = n_2/(\beta\lambda)$] is 5.7 at 720 nm, which meets the requirement of $\text{FOM} > 5$ for a Mach-Zehnder-based, all-optical switch [20]. More interestingly, the Kerr nonlinearity in ITO films can be tailored by controlling the carrier concentration. The time-resolved OKE measurements reveal that the recovery time of OKE in the ITO film is ~ 1 ps.

REFERENCES

- 1 H. Kawazoe, M. Yasukawa, H. Hyodo, M. Kurita, H. Yanagi, H. Hosono, *Nature* **389**, 939 (1997).
- 2 A. W. Metz, J. R. Ireland, J. G. Zheng, R. P. S. M. Lobo, Y. Yang, J. Ni, C. L. Stern, V. P. Dravid, N. Bontemps, C. R. Kannewurf, K. R. Poeppelmeier, T. J. Marks, *J. Am. Chem. Soc.* **126**, 8477 (2004).
- 3 K. L. Chopra, S. Major, D. K. Pandya, *Thin Solid Films* **102**, 1 (1983).
- 4 L. G. Mar, P. Y. Timbrell, R. N. Lamb, *Thin Solid Films* **223**, 341 (1993).
- 5 T. Karasawa, Y. Miyata, *Thin Solid Films* **223**, 135 (1993).
- 6 T. Ishida, H. Kobayashi, Y. Nakato, *J. Appl. Phys.* **73**, 4344 (1993).
- 7 S. Major, K. L. Chopra, *Sol. Energy Mater.* **17**, 319 (1988).
- 8 J. Hu, R. G. Gordon, *J. Appl. Phys.* **72**, 5381 (1992).
- 9 K. Zhang, F.R. Zhu, C. H. A. Huan, A. T. S. Wee, *J. Appl. Phys.* **86**, 974 (1999).
- 10 I. Hamburg, C. G. Granqvist, *J. Appl. Phys.* **60**, R123 (1986).
- 11 R. B. H. Tahar, T. Ban, Y. Ohya, Y. Takahashi, *J. Appl. Phys.* **83**, 2631 (1998).
- 12 S. A. Studenikin, M. Cocivera, *J. Appl. Phys.* **91**, 5060 (2002).
- 13 K. Zhang, F. R. Zhu, C. H. A. Huan, A. T. S. Wee, *Thin Solid Films* **376**, 255 (2000).
- 14 M. Sheik-Bahae, A.A. Said, T. Wei, D.J. Hagan, E.W. Van Stryland, *IEEE J. Quantum Electron.* **26**, 760 (1990).
- 15 Y. Sasajima, K. Taimura, *Phys Rev. B* **68**, 014204 (2003).
- 16 I. M. Catalano, A. Cingolani, A. Minafra, *Solid State Commun.* **16**, 417 (1975).
- 17 R. Adair, L. L. Chase, S. A. Payne, *Phys. Rev. B* **39**, 3337 (1989).
- 18 A. Mayer, F. Keilmann, *Phys. Rev. B* **33**, 6962 (1986).
- 19 J. He, W. Ji, G.H. Ma, S.H. Tang, E.S.W. Kong, S.Y. Chow, X.H. Zhang, Z.L. Hua, J.L. Shi, *J. Phys. Chem. B* **109**, 4373 (2005).
- 20 G. Lenz, J. Zimmerman, T. Katsufuji, M. E. Lines, H. Y. Hwang, S. Spalter, R. E. Slusher, S.-W Cheong, J. S. Sanghera, I. D. Aggarwal, *Opt. Lett.* **25**, 254 (2000).

Table 1. Electrical properties and nonlinear refractive index of ITO thin films

Film properties (Size: 1 cm × 1 cm)	Substrate (SiO ₂)	ITO-2	ITO-3	ITO-4	ITO-5
Sheet Resistance (Ω/square)	-	30.9	25.5	25.1	27.1
Carrier concentration, N _d (×10 ²⁰ cm ⁻³)	-	4.0	4.4	5.4	5.8
Mobility (cm ² /V-s)	-	42.9	36.8	32.5	29.1
Thickness (nm)	1 × 10 ⁶	118	130	138	133
Conductivity, σ (× 10 ³ S cm ⁻¹)	-	2.91	2.61	2.81	2.70
$E_g^{ind.}$ (eV)		3.05	3.08	3.11	3.15
n_2 (× 10 ⁻⁵ cm ² /GW) at λ = 720 nm	0.048	1.6	2.1	2.6	4.1
Re χ ⁽³⁾ (× 10 ⁻¹³ esu) at λ = 720 nm	0.28	15	21	25	40

Figure captions

Fig. 1. Transmission spectra of the ITO thin films coated on glass substrates. From these spectra, the absorption coefficient α , is inferred. In the inset, $(\alpha h\nu)^{1/2}$ are plotted as a function of the photon energy, $h\nu$. The thick solid lines represent the straight-line plots of $(\alpha h\nu)^{1/2}$ vs $h\nu$ for determination of the indirect-band-gap energy.

Fig. 2.(a) Open- and (b) closed-aperture Z-scans for the ITO film coated on the substrate recorded at a wavelength of 720 nm and an input irradiance of 256 GW/cm². For comparison, Z-scans of the glass substrate measured under the same conditions are also displayed. (c) Closed-aperture Z-scans of the ITO film coated on the substrate measured at 720 and 780 nm. The symbols are the experimental data. The solid lines are the best-fit curves calculated by the Z-scan theory.

Fig. 3. (a) The Kerr nonlinearity plotted as a function of the excitation irradiance for the ITO film. (b) The Kerr nonlinearity plotted as a function of the free-charged-carrier concentration in the ITO films. The symbols are the experimental data. The solid line in Figure (a) is a guide for the eye.

Fig. 4. (a) Optical Kerr effect (OKE) measurement on the ITO film coated on the substrate. For comparison, OKE measurement on the substrate is also displayed. (b) OKE measurements of the ITO film coated on the substrate with three different irradiances.

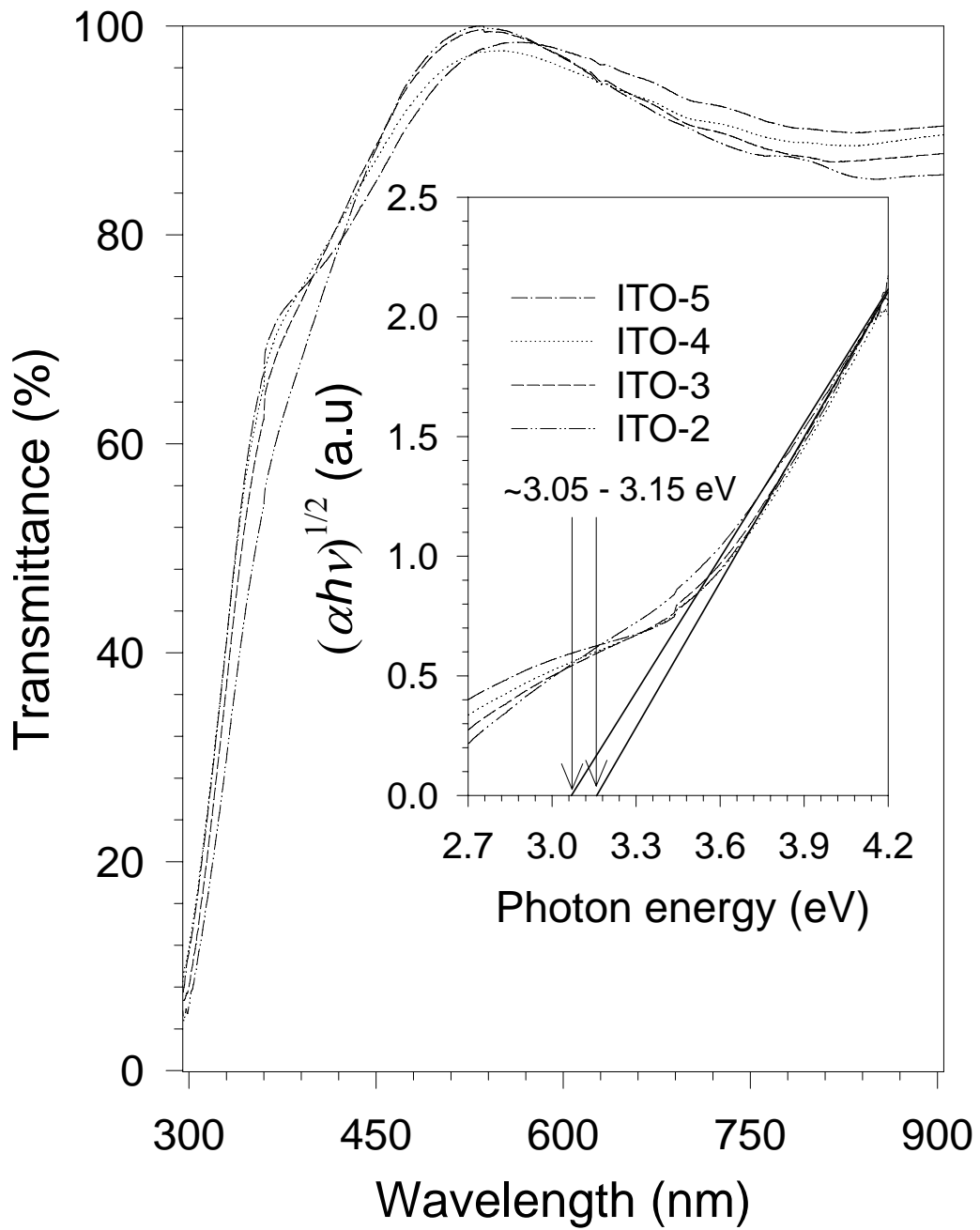


Figure 1.

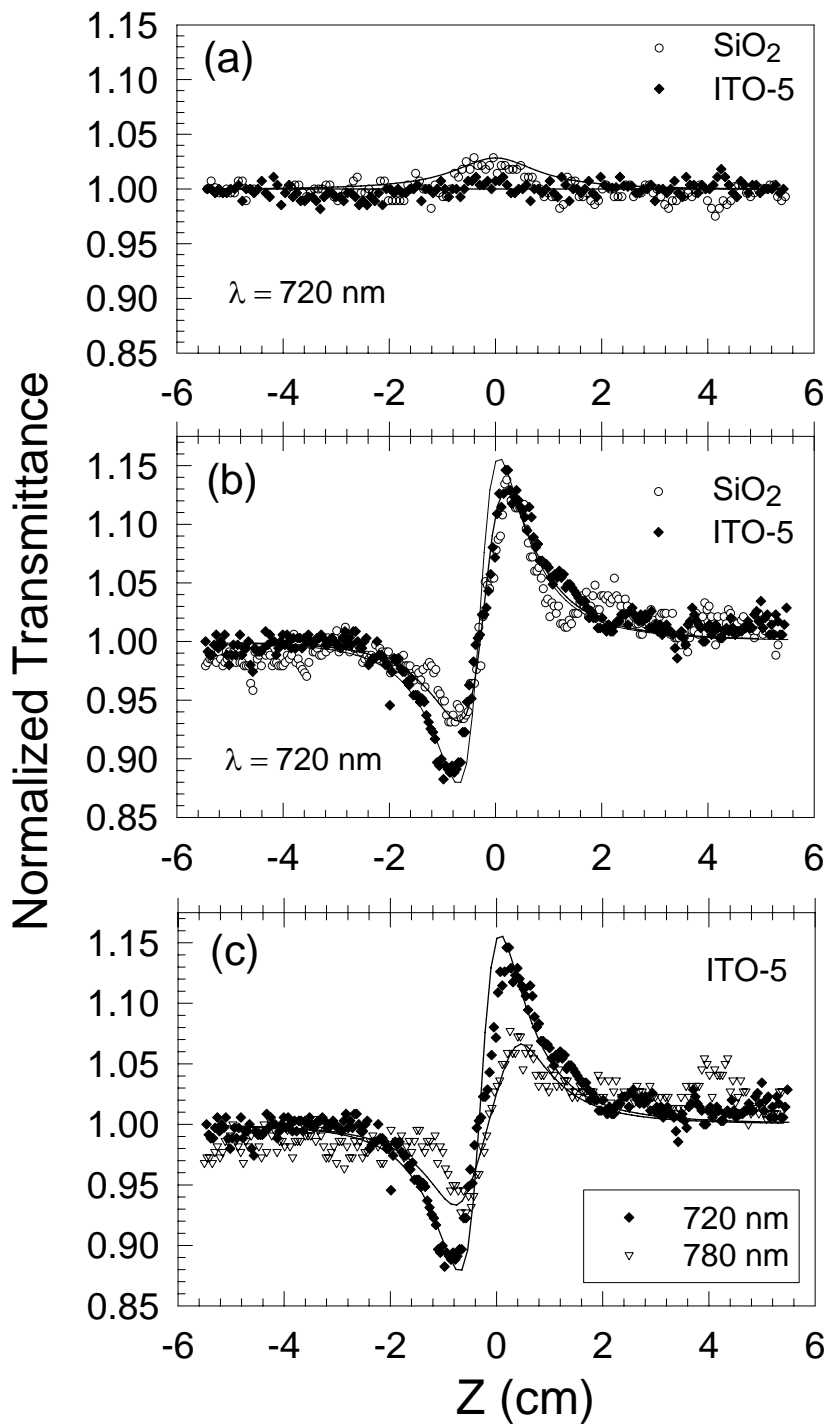


Figure 2.

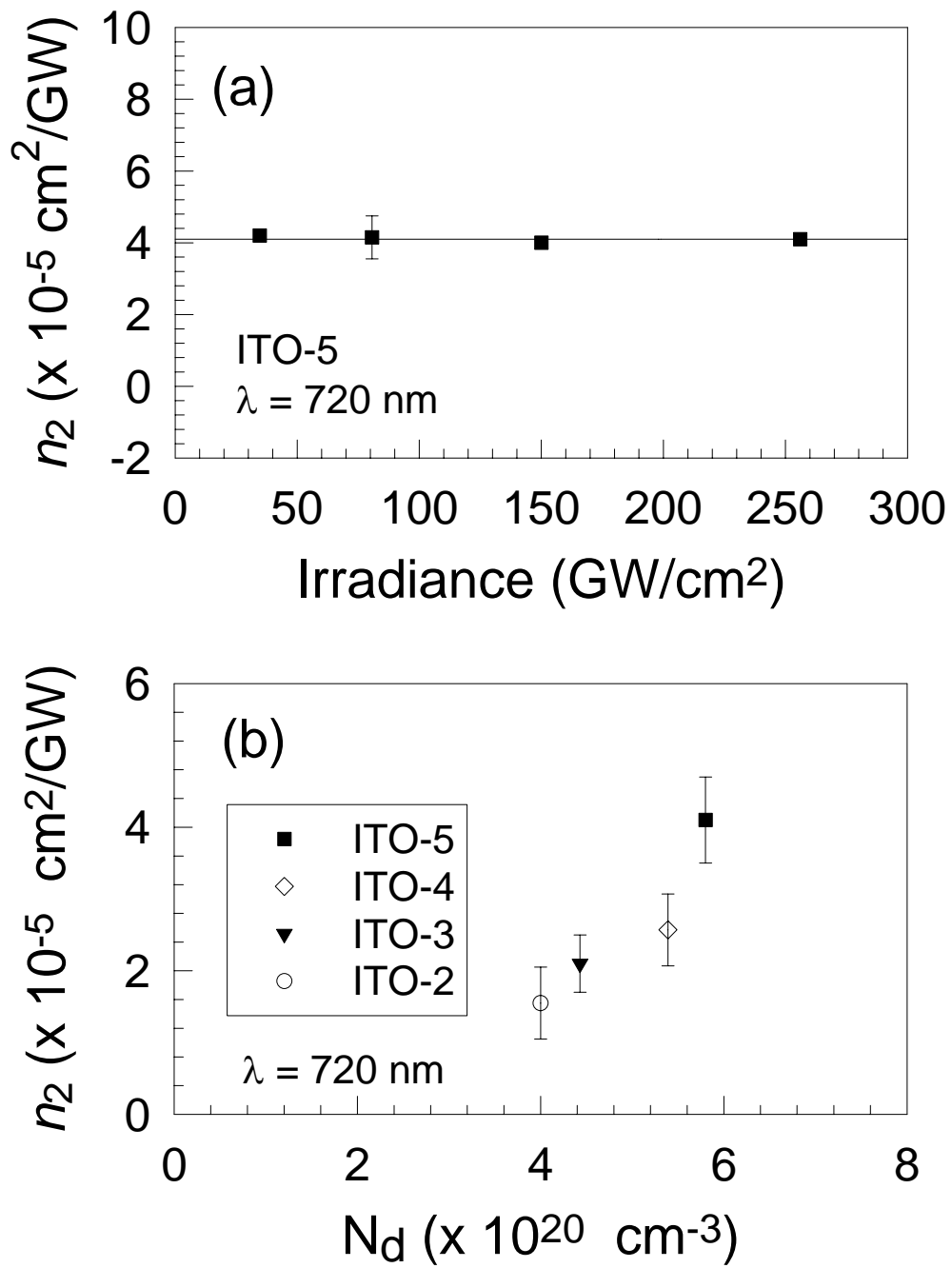


Figure 3.

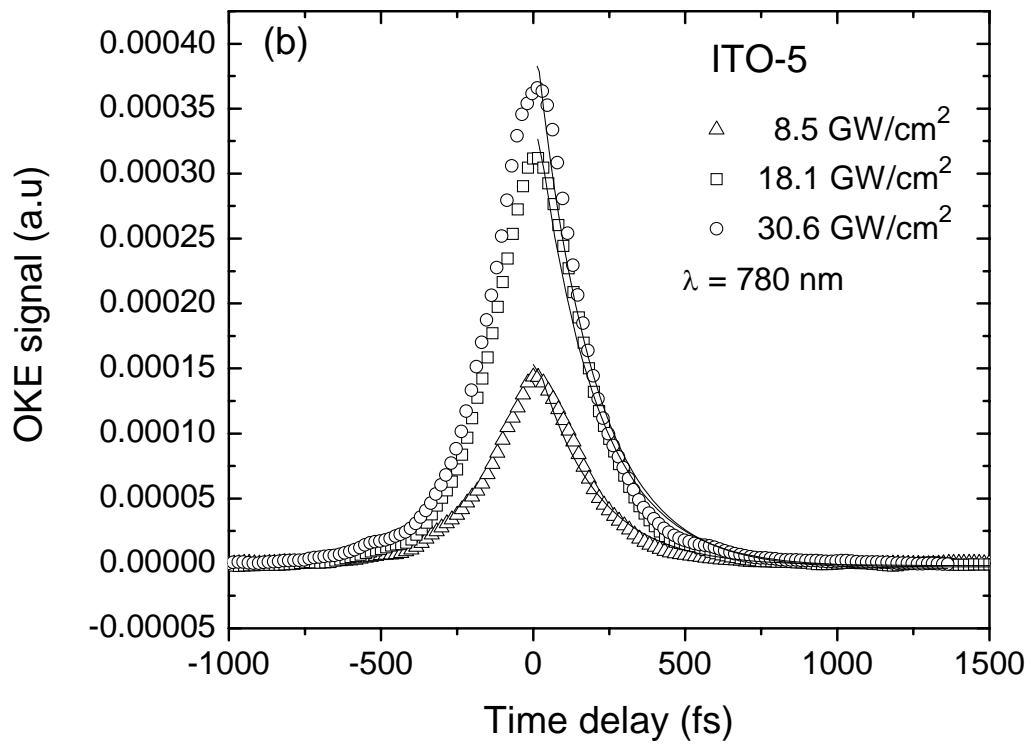
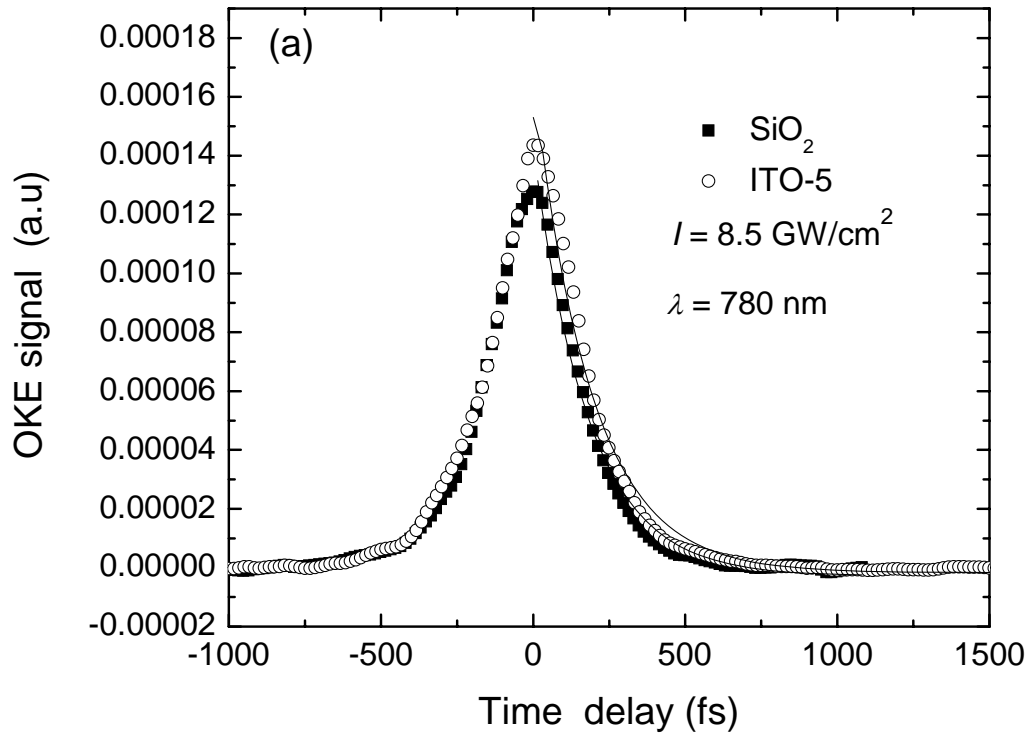


Figure 4.